Nuclear Engineering and Technology 53 (2021) 1119–1126

Contents lists available at ScienceDirect

Nuclear Engineering and Technology

journal homepage: www.elsevier.com/locate/net

Original Article

Preliminary numerical study of single bubble dynamics in swirl flow using volume of fluid method

Zhongchun Li [a, b, **], Zhifang Qiu [b], Sijia Du [a, b], Shuhua Ding [a, b], Hui Bao [b], Xiaoming Song [b], Jian Deng [b, *]

[a] Science and Technology on Reactor System Design Technology Laboratory, Nuclear Power Institute of China, Chengdu, 610041, China
[b] Nuclear Power Institute of China, Chengdu, 610041, China

ARTICLE INFO

Article history:
Received 17 March 2020
Received in revised form
13 September 2020
Accepted 26 September 2020
Available online 4 October 2020

Keywords:
Swirl flow
Spacer grid
Bubble dynamics
VOF

ABSTRACT

Spacer grid with mixing vane had been widely used in nuclear reactor core. One of the main feather of spacer grid with mixing vane was that strong swirl flow was formed after the spacer grid. The swirl flow not only changed the bubble generation in the near wall field, but also affected the bubble behaviors in the center region of the subchannel. The interaction between bubble and the swirl flow was one of the basic phenomena for the two phase flow modeling in fuel assembly. To obatin better understanding on the bubble behaviors in swirl flow, full three dimension numerical simulations were conducted in the present paper. The swirl flow was assumed in the cylindral calculation domain. The bubble interface was captured by Volume Of Fluid (VOF) method. The properties of saturated water and steam at different pressure were applied in the simulation. The bubble trajectory, motion, shape and force were obtained based on the bubble parameters captured by VOF. The simulation cases in the present study included single bubble with different size, at different angular velocity conditions and at different pressure conditions. The results indicated that bubble migrated to the center in swirl flow with spiral motion type. The lateral migration was mainly related to shear stress magnitude and bubble size. The bubble moved toward the center with high velocity when the swirl magnitude was high. The largest bubble had the highest lateral migration velocity in the present study range. The effect of pressure was small when bubble size was the same. The prelimenery simulation result would be beneficial for better understanding complex two phase flow phenomena in fuel assembly with spacer grid.

1. Introduction

Critical heat flux(CHF) is one of the most important limiting parameters in designing and operating nuclear reactor system, which results in sudden increase of wall temperature as boiling crisis occurred. Spacer grid is utilized to maintain the spacing between fuel rods and reduce the flow induced vibration. Mixing vanes are mainly utilized in PWR to promote CHF in the fuel assembly. Mixing vane on the spacer grid increases CHF significantly. The mechanisms of CHF enhancement are caused by multiple effects(Chang et al., 2006) [1]. One of the principal reason is the formation of strong swirl flow just after the spacer grid and the attenuation along the channel. The formation of swirl flow results in a significant increase of mixing of momentum and energy exchange between connected subchannel. The centrifugal force generates by the swirling motion forced the liquid rusts the heat surface, which enhances the wall heat transfer and interface exchange. Besides, the bubbles breakup into small bubble by spacer grid and move toward to the center by the lateral force, i.e. lift force which is caused by the velocity gradient in swirl flow. The swirl flow prevents bubble crowding in the cladding wall and induces bubble migrated to the center of the subchannel. Previous international benchmark exercise on turbulent mixing in a rod bundle had shown that strong swirl flow was formed downward the mixing vane (Chang et al., 2014) [2]. The maximum vorticity for swirl type and split type mixing vane reached as high as 350 s^{-1} at 1 D_H (hydraulic diameter) and gradually decayed to about 80 s^{-1} at 10 D_H. For the swirl type mixing vane, the shape of the vorticity

* Corresponding author.
** Corresponding author. Science and Technology on Reactor System Design Technology Laboratory, Nuclear Power Institute of China, Chengdu, 610041, China.
E-mail addresses: zhongchun.lee@gmail.com (Z. Li), dengjian_npic@163.com (J. Deng).

https://doi.org/10.1016/j.net.2020.09.027

Nomenclature

CHF	Critical Heat Flux
VOF	Volume Of Fluid
PLIC	Piecewise Linear Interface Calculation
CSF	Continuum Surface Force
MUSCL	Monotonic Upstream-centered Scheme for Conservation Law
PISO	Pressure Implicit with Splitting of Operator
CPD	Cell per Diameter

Symbol

D_H	hydraulic diameter
t	time
v	velocity
x	x-direction
P	Pressure
$\vec{F}_\sigma$	Surface tension force
$\vec{n}$	Norm direction

Greek Symbol

ρ	density
μ	Viscosity
σ	Surface tension
ω	Shear stress magnitude
α	Void fraction
κ	curvature

Subscript

k	Phase identification
l	liquid
g	vapor

contour was near sphere in the sub-channel center. The shape of the vorticity contour in the case of the split type was elliptic. The bubble dynamic in swirl flow, especially the lateral migration characteristics, was essential to understand the two phase flow dynamics in fuel assembly.

A lot of work has been done on the lateral migration in simple shear flow in literature, which depended on the Reynolds (Re) number, the Eotvös (Eo) number, shear rate (Sr) number, and Morton (Mo) numbers. Legendre and Magnaudet (1998) [3] studied spherical bubbles in linear shear flow. Kariyasaki (1987) [4], Ervin and Tryggvason (1997) [5], Tomiyama et al. (2002) [6] and Adoua et al. (2009) [7] found that the increase of bubble size changed the lift force direction, which explained the transition from void wall peaking to void core peak observed in pipe flows (Serizawa et al., 1975) [8]. Rastella et al.(2011) [9] obtained the bubble dynamics in horizontal rotate shear flow and the lift force was calculated based on the steady bubble position. Li et al.(2014, 2016, 2016) [10–12] investigated the bubble migration in simple shear flow with low viscosity fluid and large range of bubble diameter. Besides, Shuo Liu et al.(2018) [13] investigated the separator performance with the vane-type swirling flow in oil-gas mixture. Yin, J. et al.(2018,2019) [14,15] experimentally and theoretically studied the tiny small bubble behaviors, which were generated in online fission gas removal system in molten salt reactors. However, the bubble dynamics in swirl flow under pressurizer water reactor condition was still lack.

To get better understanding on the bubble behaviors in swirl flow, full three dimension numerical simulations using VOF(Volume of fluid) were conducted in the present paper. The motion, trajectory and shape deformation of a single bubble in swirl flow in water were analyzed. The basic computational methods, include the simulation conditions and simulation cases were presented in the subsequent section. The third section was about the discussion on effects of shear stress magnitude, the bubble size and pressure on the bubble dynamics in swirl flow. The final part was the conclusion.

2. Computational methods

2.1. VOF model

The VOF (Hirt and Nichols, 1981) [16] was applied to capture interface. In the VOF method, $\propto_k$ was applied to represent the volume ratio of the phase k in a computational cell. If $\propto_k = 1$, it indicated that the cell was filled with phase k, if $\propto_k = 0$, it indicated that the cell had no phase k. While if $0 < \propto_k < 1$, then it was the interface between phase k and other phase. The sum of phase volume fraction equaled to 1.

The interface capture was based on the solving of volume fraction field. For phase k, the continuity equation was as follows,

$$\frac{\partial(\alpha_k \rho_k)}{\partial t} + \nabla \cdot \left(\alpha_k \rho_k \vec{v}_k\right) = 0 \tag{1}$$

When the void fraction field was obtained, the interface was reconstructed by piecewise linear interface calculation (PLIC) scheme (Rider and Kothe, 1998) [17].

A single momentum equation was solved throughout the computational domain. The momentum equation was solved as follows,

$$\frac{\partial(\rho \vec{v})}{\partial t} + \nabla \cdot \rho \vec{v} \vec{v}\Big) = -\nabla p + \nabla\left[\mu \nabla \vec{v} + (\nabla \vec{v})^T\right)\Big] + \rho \vec{g} + \vec{F}_\sigma \tag{2}$$

In the equations,

$$\rho = \alpha_g \rho_g + (1-\alpha_g)\rho_l \mu = \alpha_g \mu_g + (1-\alpha_g)\mu_l \tag{3}$$

ρ_g, ρ_l, μ_g and μ_l represented the density of gas, density of liquid, viscosity of gas, viscosity of liquid. $\vec{F}_\sigma$ represented the surface tension in the interface. For the surface tension effect, the CSF(Continuum Surface Force) model (Brackbill et al., 1992) [18] was used, as it alleviated the interface topology constraints. It interpreted surface tension as a continuous, three-dimensional effect across an interface. It was defined as follows,

$$\vec{F}_\sigma = \sigma \frac{\rho \kappa \vec{n}}{1/2(\rho_g + \rho_l)}, \tag{4}$$

$\sigma$was surface tension, ρ was density defined before, $\vec{n}$ was the vector of interface, κ was the curvature and was defined as follows (Brackbill et al., 1992) [18],

$$\kappa = -(\nabla \vec{n}) = \frac{1}{|\vec{n}|}\left[\frac{\vec{n}}{|\vec{n}|}(\nabla|\vec{n}|) - (\nabla \cdot |\vec{n}|)\right] \tag{5}$$

2.2. Simulation condition

The geometry and boundary conditions used in the present paper were shown in Fig. 1. Cylinder domain was used to simulate the bubble dynamics in the swirl flow. The domain size was determined by balance of computational cost and simulation requirements, with radius of 5 mm and height of 30 mm. The inlet was set to swirl flow on the top plane with velocity distribution of $v_r = \omega r$, where ω was the angular velocity, r was the radius position. The velocity on the z and θ direction was zero. The outlet condition was set to out flow on the bottom plane. The boundary condition on the cylinder's outer surface was set to moving wall. The rotating velocity on the wall was set to equal to $V_R = \omega R$. When the bubble interacts with the swirl flow field around it under buoyancy force, the chronologically change in the flow field in the actual situation was captured under the present flow field setting. In the present simulation, no turbulence was assumed at the initial flow field and laminar flow model assumption with the nearly direct numerical simulation.

When using VOF method to conduct bubble dynamics simulation, initial bubble volume was needed for interface tracking. As the bubble interface and motion were chronologically change by the bubble-swirl flow interactions and was not able to be pre-defined, sphere bubble region was set. The initial bubble center was set on the position whose radius was 3.0 mm with enough lateral migration distance and elimination of boundary influence. The bubble center was set on z = 6 mm from the bottom plane. The initial flow field for flow and bubble was set as $v_r = \omega r$, which was the same for bubble and fluid. The bubble shape and velocity reached equilibrium state very shortly after released into the flow field. The pressure in the bubble was set as $P = P_0 + 4\sigma/d$, where P_0 was the reference pressure and d was the diameter of the bubble.The spatial derivatives were discrediting with 3 order-MUSCL scheme, while the time derivatives were using first order implicit method. For pressure and velocity coupling, the Pressure Implicit with Splitting of Operator (PISO) algorithm (Issa, 1986) [19] was applied in momentum equation.

Fig. 2. t = 39.1 ms, bubble shape of different CPDs (blue line, CPD = 12; yellow line, CPD = 15; black, CPD = 18) (Li et al. (2014)). (For interpretation of the references to colour in this figure legend, the reader is referred to the Web version of this article.)

2.3. Mesh setting and prelimenary validation

Depending on a previous study of Li et al. (2014) [10], the mesh setting in the present paper was set with a balance of accuracy and computational capacity. Fig. 2 presented bubble shape at time t = 39.1 ms with three sets of CPD (CPD = d/dx, the number of cells per diameter direction), namely, 12, 15, and 18. Bubbles with different CPD reached the same elevation on z direction and hold almost the equivalent gravity center. Bubbles of three meshes almost stayed the same as a spherical cap pattern. As simulation time is doubled with these three sets of CPD, CPD of about 15 was set for the subsequent investigation for the present simulation with sufficient accuracy.

Preliminary model validation was conducted for a free rising bubble in still water as showed in Fig. 3. The bubble was generated with a gentle-push method using capillary tube, whose diameter was 0.267 mm (Wu and Gharib (2002) [20]. Images of bubble shape at different time were recorded during the bubble deformation process. Additional cases were validated by Tomiyama.et al. (2002) experiment for lateral migration in linear shear flow. The

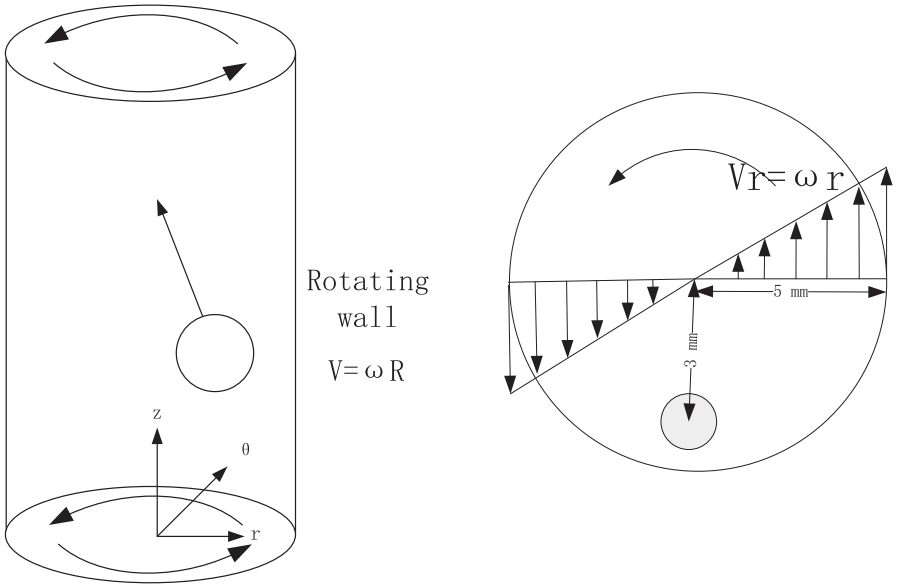

Fig. 1. Geometry and boundary condition.

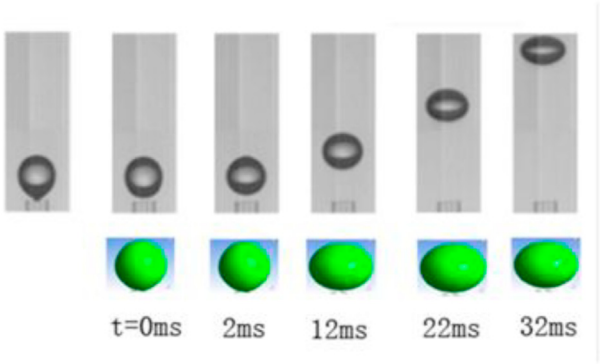

Fig. 3. Validation of simulation result (Li et al., 2014).

comparison was shown in Fig. 4, where $X^* = \frac{\bar{x}-x_0}{W}, \bar{x} = \frac{\sum \rho_g \alpha_g x}{\sum \rho_g \alpha_g}, Z^* = \frac{\bar{z}-z_0}{W}, \bar{z} = \frac{\sum \rho_g \alpha_g z}{\sum \rho_g \alpha_g}$. The almost same bubble trajectory was observed in the simulation and experiment results for bubble diameter of 2.84 mm and 5.54 mm. The VOF simulation results reached a good agreement with the experimental records(Li et al., 2014) [10].

3. Simulation case

A base case and three cases with three variable parameters were conducted to obtain the bubble dynamics in swirl flow, which were illustrated in Table 1. The detailed information of base case was set as bubble size was 1 mm, angular velocity was 100 s^{-1} and the pressure was 15.5 MPa. The reason of determination of bubble size is that the bubble with diameter of 1 mm was in oblate ellipsoidal region at base case condition with affordable computational cost, which was the most concerned region in real situation. The potential angular velocity range in the experiment of Chang et al. (2014) [2] was from 80 s^{-1} to 350 s^{-1}. To obtain the potential swirl flow's effect, three angular velocities were studied with 50 s^{-1}, 100 s^{-1} and 200 s^{-1}, respectively. Case 2 was to study the bubble diameter's effect. Three bubble diameters with diameter of 1 mm, 1.5 mm and 2 mm, respectively, were modeled. When the bubble initial diameter was raised, the mesh setting was the same. Case 3 was simulated to get the pressure's effect on the bubble dynamics. Three pressure levels at 5 MPa, 10 MPa and 15.5 MPa were investigated, which covered the most concerned regime. The properties

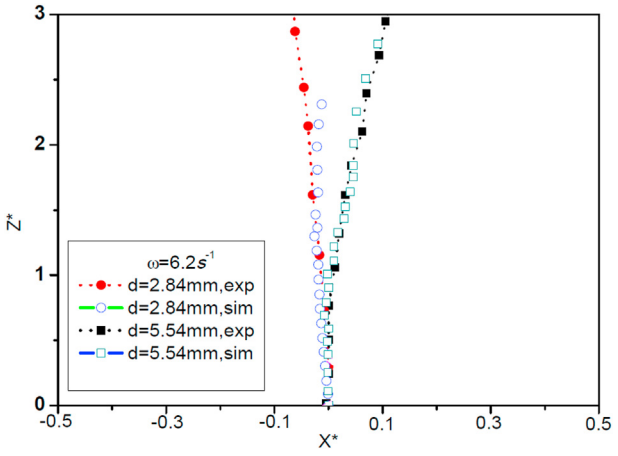

Fig. 4. Validation of simulation result with Tomiyama.et al. (2002) (Li et al., 2014).

Table 1
Simulation case.

No.	D_b(mm)	$\omega(s^{-1})$	Pressure(MPa)	Fluid
Base Case	1	100	15.5	Water
Case 1	1	50	15.5	Water
		100		
		200		
Case 2	1	100	15.5	Water
	1.5			
	2			
Case 3	1	100	5	Water
			10	
			15.5	

used for these three cases were presented in Table 2.

4. Result and discussion

4.1. Typical bubble motion

The first section presented typical bubble motion in swirl flow. The detailed parameters were given in Table 1. The bubble trajectories, velocity and shape evolution were discussed.

The three dimension bubble trajectory was illustrated in Fig. 5. The bubble rose up in a shrink spiral motion and finally reached the center of the cylindral domain. The bubble trajectory was divided into two stages. The first stage was the period before the bubble edge touched the center. The second stage was the stage when the bubble oscillated around the centerline. In the first stage, the bubble trajectory was coupled by a circular motion and lateral motion towards the cylinder center. The circular motion was caused by the swirl flow and the lateral motion was caused by the swirl induced lift force. The combination of these two mechanisms caused the shrink spiral motion. There were approximately two cycles before the bubble edge reached the center. The second stage was followed when the distance between bubble center and domain center was less than the bubble radius. The lateral force was decreased as the swirl flow experienced by the bubble decreased.

The projection of bubble trajectory on XY plane was given in Fig. 6. On the XY plane, the trajectory type was near sphere. The radius of trajectory circle was declined and finally converged into the domain center. In the first round, the trajectory radius in x direction decreased about 1 mm in each half cycle. After about two cycles, the bubble edge reached the center. When the bubble entered into the center region, it stayed into the center in an oscillate way. The distance between bubble center and the domain center was given in Fig. 7. It has three different patterns. The slopes in these three stages were reduced. The first stage ended when the distance decreased to about 0.75 mm and the slope was about 25 mm/s. The second stage ended when the distance was near the domain center and the average slope was about 6 mm/s.

The velocity evolution was shown in Fig. 8. The angular velocity monotonously decreased from the maximum value of about 0.3 m/s when bubble was at the initial position to 0 m/s when bubble was near the center region. The radial velocity was negative and increased to around 0. The velocity evolution was also divided into three stages. In the first stage, the radial velocity first decreased and then increased to a stable value. The angular velocity went down at relatively high velocity. In the second stage, radial velocity stayed at negative value and the angular velocity decreased in a linear manner. The third stage, the radial velocity slowly increased to near zero. The angular velocity was also near zero.

Shape evolution at three time points was shown in Fig. 9. As the bubble diameter was about 1 mm in the present simulation, which

Table 2
Properties used in simulation.

Fluid	Pressure	ρ_l(kgm^{-3})	μ_l(kgm^{-1} s^{-1})	ρ_g(kgm^{-3})	μ_g(kgm^{-1} s^{-1})	σ(Nm^{-1})
Water	15.5 MPa	594.4	6.83×10^{-5}	101.9	2.31×10^{-5}	0.00467
Water	10 MPa	688	8.18×10^{-5}	55.5	2.03×10^{-5}	0.012
Water	5 MPa	777.4	1.0×10^{-4}	0.5981	1.80×10^{-5}	0.02276

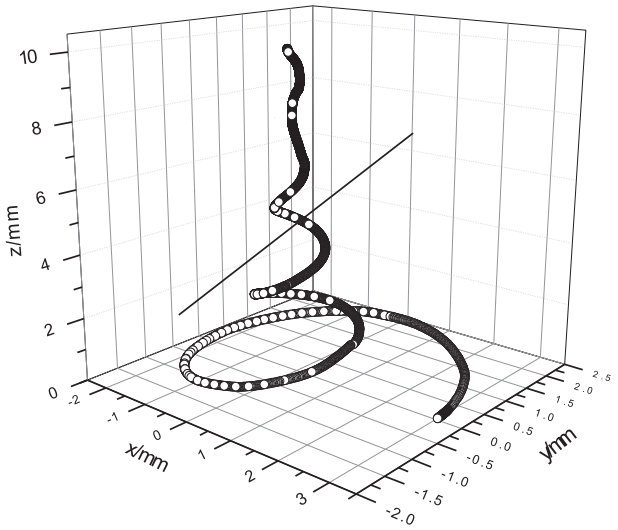

Fig. 5. 3-D bubble trajectories.

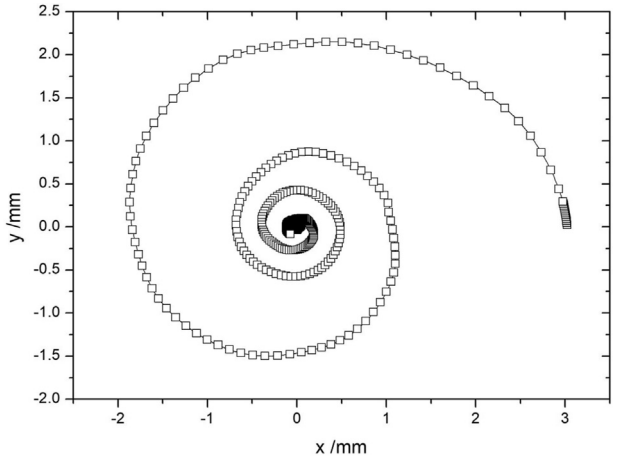

Fig. 6. Bubble trajectories projection on XY plane.

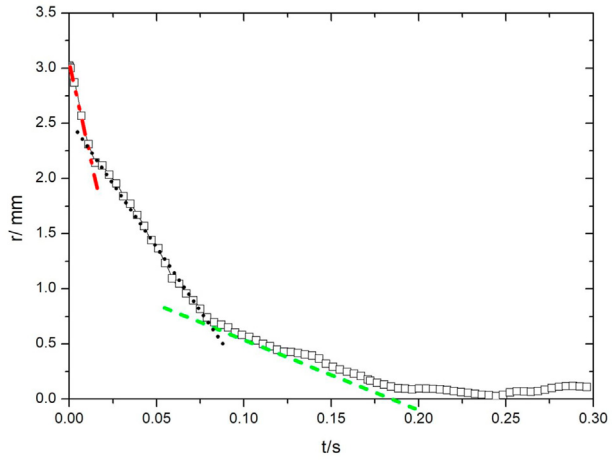

Fig. 7. Bubble center position in radius direction.

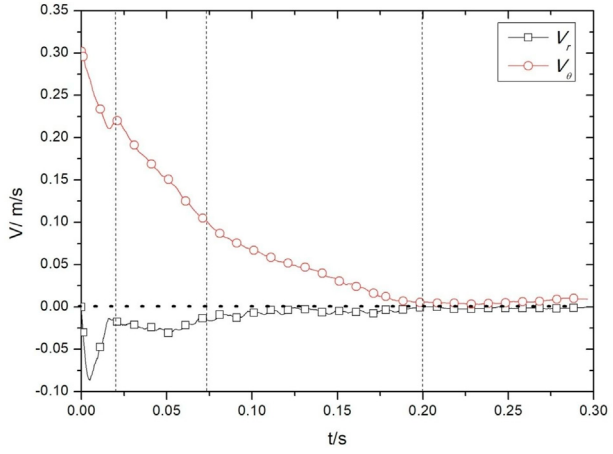

Fig. 8. Bubble velocity evolution.

was in the region of oblate ellipsoid region, the bubble was kept as oblate ellipsoid. The results revealed that the swirl flow has no significant effect on the bubble deformation.The bubble shape at different time step was similar to each other which shown that the bubble shape was also independent with bubble center position.

It confirmed that bubble migrated to the swirl flow center in shrinking spiral approach which was a combination of the lateral motion to the bubble center by lift force, the rotating route by drag force and rising up by the buoyancy force. The bubble migrated to the center quickly and stayed oblate ellipsoid shape in swirl flow. When the bubble reached the center region, the bubble remained in the region in oscillating way, which may result in bubble coalescence in this region.

4.2. Swirl flow effect

The swirl flow was directly related to the bubble behaviors and the interfacial force of bubble in shear flow as the bubble was surrounded by the liquid. It was also directly related to the mixing-vane design. The angular velocity ω is one of the most important parameter to characterize the swirl flow. Three angular velocities, with value of 50 s^{-1}, 100 s^{-1} and 200 s^{-1}, respectively, were studied. The swirl flow effect on bubble trajectories were shown in Fig. 10. The trajectory pattern was similar to the typical bubble trajectory pattern. The bubbles had the shortest migration path under the highest swirl condition. When the swirl flow was 50 s^{-1}, the migration distance was smaller, remaining larger than 1 mm even after two cycles.

The bubble velocity evolution under different swirl magnitude was presented in Fig. 11. The velocity evolution pattern for these

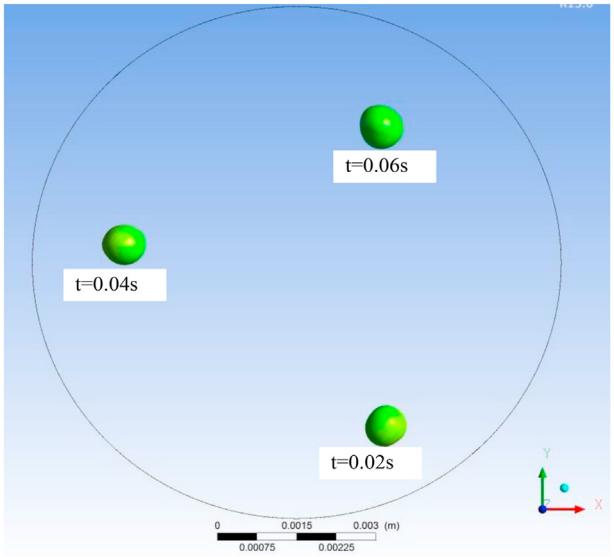

Fig. 9. Bubble shape evolution.

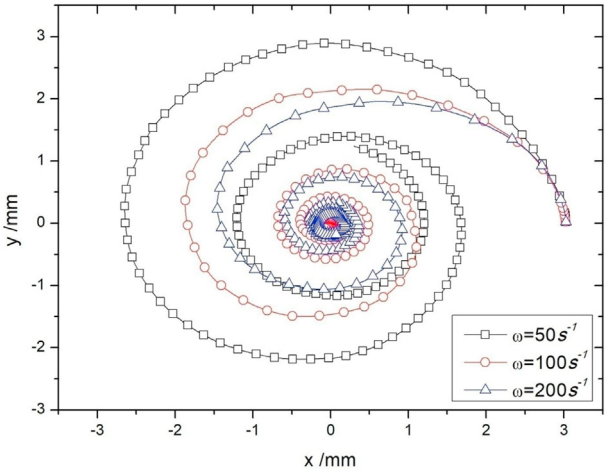

Fig. 10. Trajectory projection on XY plane.

bubbles was comparable. The frequency and amplitude of these velocities were decreased when swirl magnitude increased.

This section showed that the lateral migration characteristics were highly related to the swirl magnitude. When the swirl magnitude was larger, the bubble moved toward the center with higher velocity and shorter time. The stronger the swirl magnitude was, the faster was the bubble migrated to the center. It could be further inferred that when the stronger swirl flow generated after the mixing vane, the more probable would be the bubble migrate to the channel center region.

4.3. Bubble size effect

To ensure enough CPD in the simulation case, bubble sizes of 1 mm, 1.5 mm and 2 mm were studied in the present study. The bubble trajectories with different size were shown in Fig. 12. The biggest bubble (D_b= 2 mm) has the shortest lateral migration path and it migrated to the center region in less than 3/4 cycles. The path of bubbles with a diameter of 1.5 mm was between these two bubbles. The bubble migrated to the center region in about one

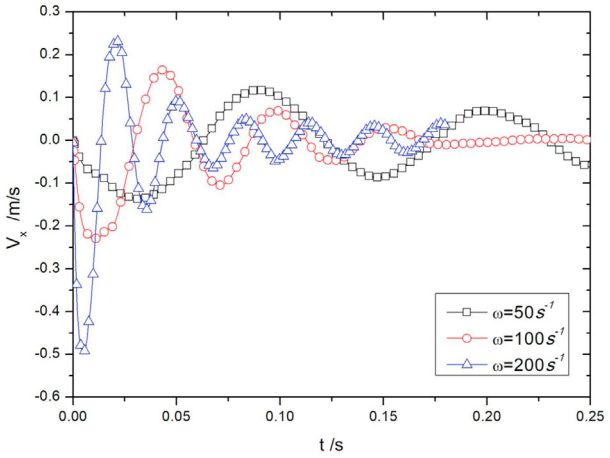

Fig. 11. Velocity evolutions at different swirl magnitude.

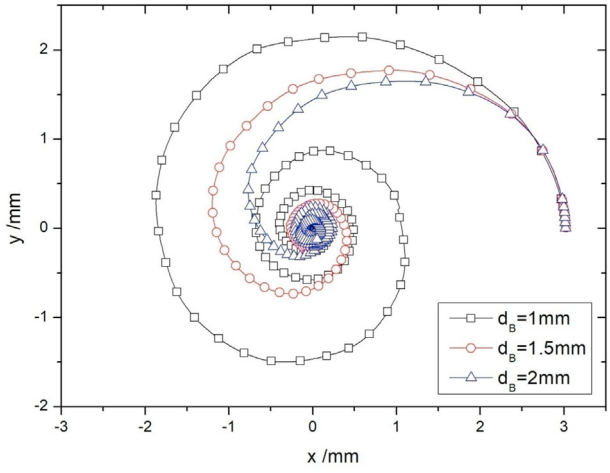

Fig. 12. Trajectory projection on XY plane.

cycle. When the bubble was in the center region, the trajectories for bubble size of 2 mm and 1.5 mm was overlapped. The bubble stayed in the center region after the bubble reached the center.

The velocity of a bubble with different size was shown in Fig. 13. The highest velocities reached by these three bubbles were almost the same at the same time. The oscillation frequencies for these bubbles were also similar to each other. From the velocity evolution, it indicated that the biggest bubble first reached the center region. The velocity of a bubble with a diameter of 1.5 mm was the same to bubble to 2 mm after 1 cycle. The typical bubble reached the center region in two cycles. All bubbles were in the center at t = 0.17s and the velocity at x axis declined to around zero.

This section showed that the bubble size was also of vital importance in the bubble dynamics in swirl flow. When the bubble diameter was greater, the bubble moved toward the center with high velocity and short distance. The bigger the bubble was, the faster the bubble migrated to the center. In real fuel assembly configuration, the bubble would breakup into small bubbles. The present study indicated that the poly dispersion effect should be treated as their different migration characteristics.

4.4. Pressure effect

The pressure was one of main parameter to determine the fluid property, such as density, viscosity and surface tension. Wide range

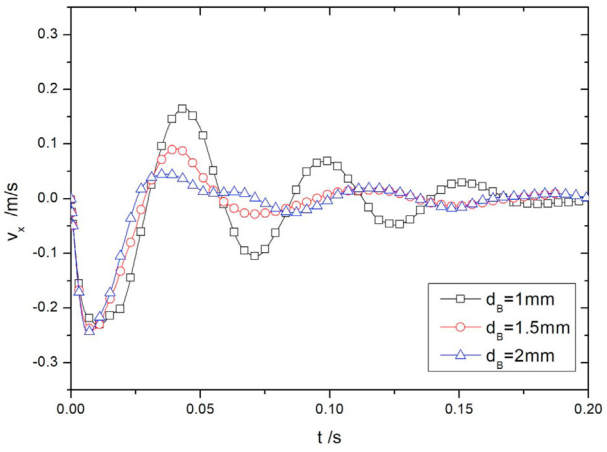

Fig. 13. Bubble velocity for different size.

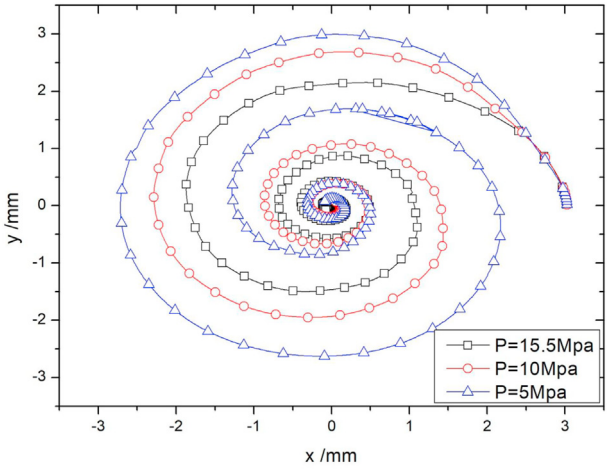

Fig. 14. Trajectory projection on XY plane.

of pressure existed in pressurizer water reactor application. Three pressure levels were invesitigated, as 5 MPa, 10 MPa and 15.5 MPa in the present study. The effect of pressure on bubble trajectories was shown in Fig. 14. The trajectories pattern was similar when bubbles were at different pressure. When the pressure is 5 MPa, the radius of bubble trajectories was bigger, which indicated that the lateral migration velocity was slightly slower. After 1 cycle, the bubble of pressure of 5 MPa, 10 MPa and 15 MPa migrated to 1 mm, 1.5 mm and 1.75 mm, respectively. When the bubble was near the center, the bubble trajectories was converged to the same line.

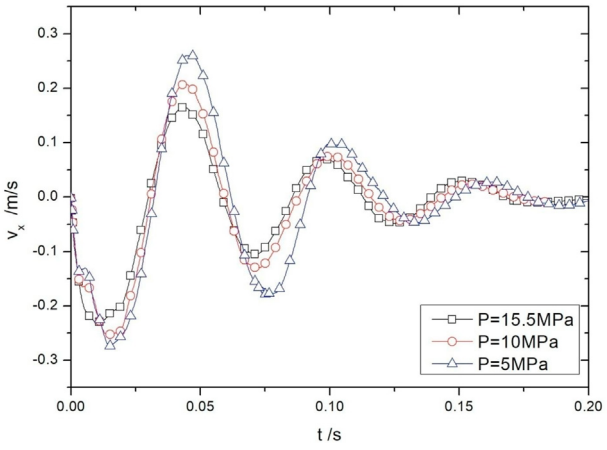

Fig. 15. Bubble velocity at different pressure.

The bubble velocity evolution under different pressure condition was illustrated in Fig. 15. The pattern and frequency for these bubbles were similar to each other. The amplitude of these velocities was decreased when pressure increased. The frequency of these velocities in each cycle was also slightly increased with pressure. When the bubble was located in the center region, the velocity of these bubbles became similar.

For the bubble of the same size in different pressure condition in swirl flow, only slightly difference was observed for bubble trajectories and bubble velocity. The pressure effect for bubble dynamics was small comparing with the effect of swirl and bubble size.

5. Conclusions

The present paper numerically studies the bubble dynamics in swirl flow, especially the lateral migration characteristics. The results confirmed that bubble was in spiral motion type with significance lateral motion. The lateral migration was mainly related to shear stress magnitude and bubble size. The bubble moved toward the center with high velocity when the swirl magnitude was high. The largest bubble had the highest lateral migration velocity in the present study range. The effect of pressure was small when bubble size was the same. The prelimenery simulation result would be beneficial for better understanding complex two phase flow phenomena in fuel assembly with spacer grid.

More work is still needed to do to better understand the mixing vane's effect on bubble dynamics, such as interaction among bubbles, turbulent flow and decay swirl flow, interactions, swirl flow induced bubble coalescence, and the poly-dispersion effect.

Declaration of competing interest

The authors declare that they have no known competing financial interests or personal relationships that could have appeared to influence the work reported in this paper.

Acknowledge

The authors would like to thank to the support of National Natural Science Foundation of China under Grant No. 11705187, 11875243.

Appendix A. Supplementary data

Supplementary data to this article can be found online at https://doi.org/10.1016/j.net.2020.09.027.

References

[1] Soon Heung Chang, Yonghoon Jeong, Byung Soo Shin, Critical heat flux enhancement, Nuclear Engineering and Technology 38 (8) (2006) 753–762.
[2] Seok-Kyu Chang, Seok Kim, Chul-Hwa Song, Turbulent mixing in a rod bundle with vaned spacer grids: OECD/NEA–KAERI CFD benchmark exercise test, Nucl. Eng. Des. 279 (2014) 19–36.
[3] Dominque Legendre, Jacques Magnaudet, The lift force on a spherical bubble in a viscous linear shear flow, Journal of Fluid Mechanism 368 (1998) 81–126.
[4] Kariyasaki, Behavior of a single gas bubble in a liquid flow with a linear velocity profile, in: Proceedings of ASME-JSME Thermal Engng Joint Conf., Honolulu Hawaii, 1987, pp. 261–267.
[5] E.A. Ervin, G. Tryggvason, The rise of bubbles in a vertical shear flow, J. Fluid Eng. 119 (1997) 443.
[6] A. Tomiyama, H. Tamai, I. Zun, S. Hosokawa, Transverse migration of single

bubbles in simple shear flows, Chem.Engng Sci. 57 (2002) 1849–1859.
[7] R. Adoua, D. Legendre, J. Magnaudet, Reversal of the lift force on an oblate bubble in a weakly viscous shear flow, J. Fluid Mech. 628 (2009) 23–41.
[8] Akimi Serizawa, Isao Kataoka, Itaru Michiyoshi, Turbulence structure of air-water bubbly flow–2. Local properties, Int. J. Multiphas. Flow 2 (1975) 235–246.
[9] Marie Rastello, Jean-Louis Marié, Michel Lance, Drag and lift forces on clean spherical and ellipsoidal bubbles in a solid body rotating flow, J. Fluid Mech. (2011) 434–459.
[10] Zhongchun Li, Xiaoming Song, Shengyao Jiang, Jiyang Yu, Numerical investigation on lateral migration and lift force of single bubble in simple shear flow in low viscosity fluid using volume of fluid method, Nucl. Eng. Des. 274 (2014) 154–163.
[11] Zhongchun Li, Yang Zhao, Xiaoming Song, et al., Experimental investigation of single small bubble motion in linear shear flow in water, Nucl. Eng. Des. 305 (2016) 334–346.
[12] Zhongchun Li, Xiaoming Song, Shengyao Jiang, et al., The lateral migration of relative large bubble in simple shear flow in water, Exp. Therm. Fluid Sci. 77 (2016) 144–158.
[13] Shuo Liu, Le-le Yang, Dong Zhang, et al., Separation characteristics of the gas and liquid phases in a vane-type swirling flow field, Int. J. Multiphas. Flow 107 (2018) 131–145, 2018.
[14] J. Yin, Y. Qian, T. Zhang, D. Wang, Numerical investigation on the bubble separation in a gas-liquid separator applied in TMSR, Ann. Nucl. Energy 114 (2018) 122–128.
[15] J. Yin, Y. Qian, Y. Ma, et al., Numerical and experimental study on an isolated bubble in the swirling separator, Nucl. Eng. Des. 350 (2019) 107–115.
[16] C.W. Hirt, B.D. Nichols, Volume of fluid (VOF) method for the dynamics offree boundaries, J. Comput. Phys. 39 (1981) 201–225.
[17] W.J. Rider, D.B. Kothe, Reconstructing volume tracking, J. Comput. Phys. 141 (1998) 112–152.
[18] J.U. Brackbill, D.B. Kothe, C. Zemach, A continuum method for modelingsurface tension, J. Comput. Phys. 100 (1992) 335.
[19] R.I. Issa, Solution of the implicitly discretised fluid flow equations by operatorsplitting, J. Comput. Phys. 62 (1986) 40–65.
[20] Mingming Wu, Morteza Gharib, Experimental studies on the shape and pathof small air bubbles rising in clean water, Phys. Fluid. 14 (7) (2002) 49–52.